interconversion is not suggested by the results of Murmann and colleagues.[5] For aquation studies, providing the Mo's behave independently, isomers i and ii would be expected to give uniphasic (statistical) kinetics[23-25] and not the behavior observed. Isomer iii is likewise unable to explain the rate constant pattern for $Mo_3O_4(NCS)_2^{2+}$ and $Mo_3O_4(NCS)^{3+}$. The remaining formulations, iv (for which there are two isomers) and v, provide reasonable explanations, although it is not clear how occupancy of the x position comes about. If isomerization is the result of the second substitution occurring at the same Mo, which would favor isomer v, then microscopic reversibility requires that the reverse events must occur in the aquation process. However it is less likely that a second substitution occurs at the same Mo since that Mo will already have four negatively charged ligands coordinated to it. Single y and x occupancy might be favored because separation of the two negatively charged NCS^- ligands will be maximized. However, this then raises the question as to whether the Mo sites are behaving as three equivalent independent sites. A mixture of isomers including isomers i-iii may of course be present and may contribute to the effects observed. We were unable to separate into different forms the $Mo_3O_4(NCS)^{3+}$ and $Mo_3O_4(NCS)_2^{2+}$ bands in further ion-exchange experiments. The amplitude of absorbance changes for the first and second aquation steps of $Mo_3O_4(NCS)_2^{2+}$ are about equal in magnitude. The possibility of using NMR to comment further on these effects is currently being explored.

(23) Armstrong, F. A.; Henderson, R. A.; Sykes, A. G. *J. Am. Chem. Soc.* **1980**, *102*, 6545.
(24) Marty, W.; Espenson, J. H. *Inorg. Chem.*, in press.
(25) Buckingham, D. A.; Francis, D. J.; Sargeson, A. M. *Inorg. Chem.* **1974**, *13*, 2630.

Equilibrium constants for (1:1) complexing from k_1 and k_{-1} values in Table III are 498 (2 M HPTS), 546 (2 M HTFMS), and 987 M^{-1} (2 M $HClO_4$) at 25 °C. The equilibration experiment referred to in Table I can be used to calculate K_1, K_2, and K_3, assuming that the low-charged species (15%) is $Mo_3O_4(NCS)_3^+$. The calculated molarity of free NCS^- is 3.2×10^{-3} M, so that $K_1 = 490$ M^{-1} in agreement with the kinetic value of 498 M^{-1} in Table III. From product analyses indicated in Table III, relative values of the equilibrium constants $K_1:K_2:K_3$ are 1.5:1:0.47 whereas for a statistical relationship ratios 3:1:0.33 would be expected to apply. Also $(\epsilon_1 - \epsilon_0)$ should be equal to $1/2(\epsilon_2 - \epsilon_0)$ (the subscripts refer to the number of thiocyanates bound), and this does not seem to be the case from the information obtained. This draws attention to the involvement of x and y positions and again raises the question as to whether the x substituent is generated directly or by isomerization. For the highest NCS^- concentration (4×10^{-3} M), the equilibrium constant K_1 indicates ~67% 1:1 complexation to $Mo_3O_4^{4+}$. Some further anation to give the 2:1 thiocyanato product would be expected to contribute at this stage, which is not apparent in kinetic plots consistent with a statistical situation applying. At $[NCS^-] = 5 \times 10^{-3}$ M reduced linearity (to 75%) in kinetic plots is observed, from which point runs become increasingly biphasic with increasing $[NCS^-]$.

Acknowledgment. We are particularly indebted to Professor E. L. King for his most helpful comments and correspondence, to Professor R. K. Murmann for information prior to publication,[5] and to Professors J. H. Espenson and R. G. Pearson for comments. SERC postgraduate (A.B.S) and postdoctoral (D.T.R.) support is gratefully acknowledged.

Registry No. $Mo_3O_4(H_2O)_9^{4+}$, 74353-85-8; $Mo_3O_4(H_2O)_7(NCS)_2^{2+}$, 97059-48-8; $Mo_3O_4(H_2O)_8(NCS)^{3+}$, 97042-91-6; NCS, 302-04-5.

Contribution from the Department of Chemistry, William Marsh Rice University, Houston, Texas 77251

Kinetics and Equilibria for Reactions of the Hexachloroiridate Redox Couple in Nitrous Acid

M. S. RAM and DAVID M. STANBURY*

Received December 19, 1984

The equilibria, kinetics, and mechanisms of the reactions of the $IrCl_6^{2-/3-}$ redox couple in nitrous acid have been investigated in aqueous solution at 25.0 °C in nitric and perchloric acid media by conventional and stopped-flow spectrophotometry. In 1 M $HClO_4$, when $IrCl_6^{3-}$ and HNO_2 are mixed, the equilibrium $HNO_2 + H^+ + IrCl_6^{3-} \rightleftarrows NO + H_2O + IrCl_6^{2-}$ is established in a few milliseconds, with $+d[IrCl_6^{2-}]/dt = k_f[H^+][HNO_2][IrCl_6^{3-}] - k_r[NO][IrCl_6^{2-}]$, where $k_f = 1.8 \times 10^4$ M^{-2} s^{-1} and $k_r = 1.4 \times 10^6$ M^{-1} s^{-1}. At high $[HNO_2]$, this reaction precedes a slow loss of $IrCl_6^{2-}$ that is due to formation of NO_3^-. In 1 M NO_3^- with $[HNO_2] > [IrCl_6^{3-}]$ the rapid equilibrium is followed by zero-order formation of $IrCl_6^{2-}$, and with $[IrCl_6^{3-}] > [HNO_2]$ the process is autocatalytic. When $IrCl_6^{2-}$ is mixed with N(III) at pH ≥2, $IrCl_6^{2-}$ is consumed with rates that increase with acidity; at pH <2 the rates become less, the kinetics become non first order, and $IrCl_6^{2-}$ is only partially consumed. All of these phenomena have been accurately simulated by numerical integration of the set of differential equations that arise from k_f and k_r as defined above and several previously established processes intrinsic to nitrous acid/nitric acid mixtures. The k_f step is interpreted as rate-limiting diffusion-controlled electron transfer from $IrCl_6^{3-}$ to NO^+. The reaction of NO_2 with $[Fe(TMP)_3]^{2+}$ (TMP = 3,4,7,8-tetramethylphenanthroline), observed directly by pulse radiolysis, has a rate constant of 1.0×10^7 M^{-1} s^{-1}; this rate constant, in conjunction with the results of a prior study of the reaction of NO_2^- with $[Fe(TMP)_3]^{3+}$, has confirmed the choice of thermodynamic data used to analyze the $IrCl_6^{2-/3-}$ reactions.

Introduction

This is the second of our reports on the behavior of substitution-inert one-electron redox couples in aqueous nitrous acid. The first report, which described the reactions of $[Fe(TMP)_3]^{2+/3+}$ (TMP = 3,4,7,8-tetramethylphenanthroline), showed that reaction 1 was central in the mechanism.[1] No evidence could be found

$$[Fe(TMP)_3]^{2+} + NO_2 \rightleftarrows [Fe(TMP)_3]^{3+} + NO_2^- \quad (1)$$

for a significant role being played by the nitrosonium ion as in eq 2. Reaction 2 was eagerly sought, because of the expectation

$$[Fe(TMP)_3]^{2+} + NO^+ \rightleftarrows [Fe(TMP)_3]^{3+} + NO \quad (2)$$

that nuclear tunneling would have a major influence on its rate constant.

In continuation of the search for a reaction proceeding through a NO^+/NO pathway, as in eq 2, the $IrCl_6^{2-/3-}$ system was selected because it is anionic, it has a higher reduction potential, and it has a lower self-exchange rate than the $[Fe(TMP)_3]^{2+/3+}$ system. This system has proven to be remarkably complex, with analytical solutions to the kinetics only under quite limited conditions. However, by means of numerical integration the entire gamut of

(1) Ram, M. S.; Stanbury, D. M. *J. Am. Chem. Soc.* **1984**, *106*, 8136.

0020-1669/85/1324-2954$01.50/0

phenomena has been simulated, and the NO^+/NO pathway has been found to play a prominent role.

Experimental Section

Reagents and Solutions. Lithium perchlorate ($LiClO_4 \cdot 3H_2O$) and lithium nitrate ($LiNO_3 \cdot 3H_2O$) were prepared by neutralizing lithium carbonate (Li_2CO_3) (Baker) with concentrated $HClO_4$ and concentrated HNO_3. The salts were recrystallized by dissolving them in a minimum amount of hot water and refrigerating the resulting solution. The salts were washed with a minimum amount of ethanol and then with ether. Sodium nitrite ($NaNO_2$) and sodium pyrophosphate ($Na_4P_2O_7 \cdot 10H_2O$) were recrystallized as described earlier.[1] Sodium hexachloroiridate(IV) ($Na_2IrCl_6 \cdot 6H_2O$) (Alfa) was found to be pure by comparison of visible spectra,[2] and it was used as received. K_2IrBr_6 was available from a previous study.[3] $[Fe(TMP)_3]SO_4$ (GFS) (TMP = 3,4,7,8-tetramethylphenanthroline) was used as received.

Sodium hexachloroiridate(III) (Na_3IrCl_6) prepared by the method of Poulson and Garner[2] was contaminated with nitrite; it was instead prepared by hydrazine reduction of Na_2IrCl_6:[4]

$$4Na_2IrCl_6 + N_2H_6Cl_2 + 4NaCl \rightarrow 4Na_3IrCl_6 + N_2 + 6HCl \quad (3)$$

In a typical procedure, 750 mg (1.3 mmol) of $Na_2IrCl_6 \cdot 6H_2O$ was mixed with 35 mg (0.33 mmol) of $N_2H_6Cl_2$ and 80 mg (1.3 mmol) of NaCl and the mixture heated in 20 mL of 95% ethanol at 70 °C for 45 min. After the reaction mixture was cooled, about 50 mL of ether was added to precipitate the Na_3IrCl_6. The product was loaded on a Dowex 1-X8-200 anion-exchange column, which had previously been washed with concentrated HCl and distilled water. $IrCl_6^{3-}$ was eluted with 8 M HCl and rotary evaporated to an oil. A saturated solution of 420 mg of $NaClO_4 \cdot H_2O$ in absolute ethanol was added to precipitate $Na_3IrCl_6 \cdot xH_2O$. The anhydrous product was obtained by drying at room temperature under vacuum over P_2O_5. Its purity was checked by chlorine oxidation to $IrCl_6^{2-}$.[5] When a sample of the product was added to a solution of $IrCl_6^{2-}$, no absorbance decrease in $IrCl_6^{2-}$ was found, thus showing the absence of hydrazine or other reducing impurities. This anion-exchange method could not be applied to the purification of Na_3IrCl_6 prepared by the nitrite reduction method[2] because of the reaction of N(III) with $IrCl_6^{3-}$ in acidic media.

Solutions of $Na_2IrCl_5(H_2O)$ were obtained by the method of Littler[6] by heating a solution of Na_3IrCl_6 at 50 °C for 2 h. The product was analyzed by its visible spectrum after oxidation with chlorine in acid solution.[5]

Solutions of $IrBr_6^{3-}$ were obtained by in situ reduction of K_2IrBr_6 with $NaNO_2$ solutions. These solutions were found to undergo aquation rapidly and were used immediately after preparation.

All solutions were prepared with distilled water, were permitted to contact only glass, Teflon, and platinum, and were sparged with argon that had been scrubbed free of oxygen in a Cr^{2+} tower. Nitric oxide, when used, was handled as described previously;[1] solutions saturated at 1 atm of NO were assumed to have $[NO] = 1.9 \times 10^{-3}$ M.[7]

Analyses. Lithium perchlorate and lithium nitrate solutions were standardized by cation exchange with the H^+ form of Dowex 50W-X8 cation exchanger followed by titration against standard 0.1 M NaOH solution.

Sodium nitrite solutions were prepared and standardized as described earlier.[1]

The pH of the solutions was measured by using a Corning 130 pH meter calibrated with standard pH solutions, and UV–vis spectra were recorded on a Cary 210 spectrophotometer with 1-cm quartz cells.

The $IrCl_6^{2-}$ concentrations were determined from the absorbances at 487 nm ($\epsilon = 4100$ M^{-1} cm^{-1}).[2] The $IrCl_6^{3-}$ concentrations were determined by oxidation with chlorine[5] and measuring the $IrCl_6^{2-}$ formed as described above.

For the attempted determination of N_2O, deoxygenated solutions of Na_3IrCl_6 and $NaNO_2$ were allowed to react with deoxygenated solutions of $HClO_4$ in a deoxygenated vial. The vapor above the solution was transferred by syringe to a Finnigan 3300 GC-mass spectrometer equipped with a Spherocarb column. The instrument was calibrated with diluted solutions of saturated N_2O (2.4×10^{-2} M).[8] The ion current at m/e 30 was used for N_2O determination, instead of the ion current at m/e 44, in order to distinguish N_2O from CO_2.

The stoichiometry of the reaction of $IrCl_6^{2-}$ with N(III) at pH 2 was examined as a brief verification of prior results obtained at neutral pH.[12] A stock solution containing 25.9 mg of $Na_2IrCl_6 \cdot 6H_2O$ (4.6×10^{-3} M), 3.2 g of $LiClO_4 \cdot 3H_2O$, and 0.2 mL of 1.0 M $HClO_4$ was made up to 10 mL in a volumetric flask and deoxygenated with argon. A 5-mL sample of this was added to 5 mL of deoxygenated 4.0×10^{-4} M $NaNO_2$ solution. After 20 min, the reaction mixture was diluted 6-fold and the absorbance measured. The loss in absorbance relative to the stock solution diluted 12-fold was 0.265 A, which corresponds to a consumption of 3.9×10^{-4} M $IrCl_6^{2-}$ in the reaction mixture.

Kinetics Methods. Kinetics data were collected at 487 nm ($\epsilon_{IrCl_6^{2-}} = 4100$ M^{-1} cm^{-1}, $\epsilon_{IrCl_6^{3-}} = 17$ M^{-1} cm^{-1}) at 25.0 °C by using the stopped-flow apparatus as described previously;[3,9] the observation path length was 1 cm. For those reactions that were exponential over their entire course as determined by the linearity of their semilog plots, pseudo-first-order rate constants, k_{obsd}, were obtained by using an exponential fitting routine.

The reactions of $IrCl_6^{2-}$ with N(III) were performed at $\mu = 1.0$ M ($LiClO_4$) in the pH range 0–7 with N(III) in large excess over $IrCl_6^{2-}$ ($[IrCl_6^{2-}]_0 = 5.0 \times 10^{-5}$ M). Pyrophosphate buffer ($pK_2 = 4.8$)[10] at 5.0×10^{-4} was used for pH >5, nitrite buffer ($pK_a = 2.9$)[11] at 1.0×10^{-3}–4.0×10^{-2} M was used in the pH range 2–5, and dilute perchloric acid solutions were used below pH 2.

Reactions of $IrCl_6^{3-}$ with N(III) were carried out at $\mu = 1.0$ M ($HClO_4$–$LiClO_4$) and $\mu = 2.0$ M (HNO_3–$LiNO_3$) in the acidity range $[H^+] = 0.1$–2.0 M. In perchlorate media, the concentration of HNO_2 were limited by the dead time of the stopped flow (≈4 ms) and by the desire to maintain a flooding excess of N(III). In all the studies of $IrCl_6^{3-}$ the reactions were initiated by mixing a solution of acid with a solution of $IrCl_6^{3-}$ and nitrite.

The rapid equilibrium, attained in mixtures of N(III) with $IrCl_6^{3-}$, appeared to proceed to a further extent in a subsequent oxygen-dependent process in the stopped flow; because of the oxygen permeability of the Teflon tubing in the Aminco system, this effect could not be entirely eliminated. With oxygen-saturated solutions, the reaction reached about 80% completion in 1 M acid, but only through a slower reaction than the initial "prompt" reaction. When the reaction was performed anaerobically in an all-glass hand-stopped-flow apparatus on the Cary instrument, the rapid equilibrium step reached ≈20% completion, and was too fast to observe, but the oxygen-dependent phase was eliminated. When the reactions were done with $IrCl_6^{3-}$ in excess over HNO_2, the effect of oxygen was even more dramatic: in air-saturated solutions, the apparent $\Delta[IrCl_6^{3-}]:\Delta[HNO_2]$ stoichiometry exceeded 4:1. An explanation for these phenomena may be that HNO_2 induces the autoxidation of $IrCl_6^{3-}$.

Pulse-radiolysis studies were performed as described previously,[4] in a 1.8-cm cell at room temperature (~23 °C). Solutions of $NaNO_2$ and $[Fe(TMP)_3]SO_4$ were prepared in conductivity water and were sparged with N_2O. Transient absorbance measurements were made at 665 and 370 nm. Dosimetry was performed by using the SCN^- method.

Results

$IrCl_6^{2-}$ Reactions. The consumption ratio for the reaction of $IrCl_6^{2-}$ with NO_2^- has previously been examined at neutral pH and reported as $\Delta[IrCl_6^{2-}]/\Delta[NO_2^-] = 2.08$.[12] Current results with $[IrCl_6^{2-}]_0 = 2.3 \times 10^{-3}$ M and $[NaNO_2] = 2.0 \times 10^{-4}$ M, at pH 2, indicate $\Delta[IrCl_6^{2-}]/\Delta[NO_2^-] = 2.0$ (±0.2). On reoxidation of the product with chlorine, the original $IrCl_6^{2-}$ was obtained, thus indicating the absence of substitution products such as $IrCl_5(H_2O)^-$ and $IrCl_5(NO)^-$.[13] The net reaction can be represented by eq 4.

$$2IrCl_6^{2-} + HNO_2 + H_2O \rightarrow 2IrCl_6^{3-} + NO_3^- + 3H^+ \quad (4)$$

The reaction went to completion at pH ≥2. At pH ≥3, the reactions gave good pseudo-first-order kinetics. At pH 2, the semilog plots showed slight deviations from linearity consistent with less than first-order kinetics; a typical example is shown in Figure 1. The rate constants increased with acidity in the pH

(2) Poulson, J. A.; Garner, C. S. *J. Am. Chem. Soc.* **1962**, *84*, 2032.
(3) Stanbury, D. M.; Lednicky, L. A. *J. Am. Chem. Soc.* **1984**, *106*, 2847.
(4) Stanbury, D. M. *Inorg. Chem.* **1984**, *23*, 2879.
(5) Novoselov, R. I.; Muzykantova, Z. A. *Russ. J. Inorg. Chem.* (*Engl. Transl.*) **1970**, *15*, 1606.
(6) Cecil, R.; Littler, J. S.; Easton, G. *J. Chem. Soc. B* **1970**, 626.
(7) Schwartz, S. E.; White, W. H. *Adv. Environ. Sci. Eng.* **1981**, *4*, 1; *Chem. Abstr.* **1982**, *96*, 41697*h*.
(8) Markham, A. E.; Kobe, K. A. *J. Am. Chem. Soc.* **1941**, *63*, 449.
(9) Lednicky, L. A.; Stanbury, D. M. *J. Am. Chem. Soc.* **1983**, *105*, 3098.
(10) "Handbook of Chemistry and Physics", 62nd ed.; CRC Press: Boca Raton, FL, 1982; p D-144.
(11) Smith, R. M.; Martell, A. E. "Critical Stability Constants"; Plenum Press: New York, 1976; Vol. 4, p 47.
(12) Wilmarth, W. K.; Stanbury, D. M.; Byrd, J. M.; Po, H. N.; Chua, C.-P. *Coord. Chem. Rev.* **1983**, *51*, 155.
(13) Bottomley, F.; Clarkson, S. G.; Tong, S.-B. *J. Chem. Soc., Dalton Trans.* **1974**, 2344.

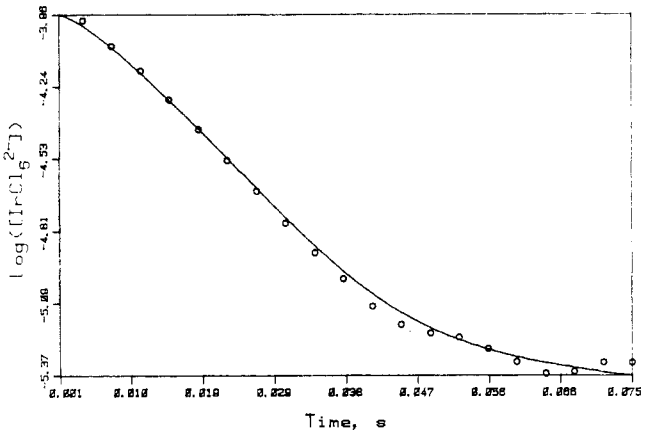

Figure 1. "Normal" kinetics for the reaction of $IrCl_6^{2-}$ with N(III) in weakly acidic media: pH 2.0, 1.0 M $LiClO_4$, $[IrCl_6^{2-}]_0 = 1.1 \times 10^{-4}$ M, $[HNO_2] = 4.0 \times 10^{-2}$ M. Solid line is a simulation.

Table I. Kinetics Data for $IrCl_6^{2-}$–N(III) Reactions[a]

$[HNO_2]$, M	pH	k_{obsd}, s^{-1}	$[HNO_2]$, M	pH	k_{obsd}, s^{-1}
6.0×10^{-2}	2.0	1.31×10^2	4.0×10^{-2}	3.47	2.6×10^b
4.1×10^{-2}	2.0	8.5×10	4.0×10^{-2}	4.02	7.9^b
4.0×10^{-2}	2.0	7.0×10	4.1×10^{-2}	5.0	1.96^b
2.0×10^{-2}	2.0	2.0×10	4.1×10^{-2}	5.8	$1.05^{b,c}$
1.0×10^{-2}	2.0	6.5	4.1×10^{-2}	6.8	$1.05^{b,c}$
4.0×10^{-3}	2.0	2.0	4.3×10^{-4}	2.0	$9.9 \times 10^{-2\,b}$
2.1×10^{-3}	2.0	1.0	4.3×10^{-4}	2.5	$4.4 \times 10^{-2\,b}$
3.6×10^{-2}	3.0	3.3×10	4.3×10^{-4}	3.0	$1.58 \times 10^{-2\,b}$
8.8×10^{-3}	3.0	1.9	4.3×10^{-4}	4.0	$1.16 \times 10^{-2\,b}$
2.2×10^{-3}	3.0	0.22	4.3×10^{-4}	5.0	$1.12 \times 10^{-2\,b}$
4.1×10^{-2}	2.5	6.4×10^b	4.3×10^{-4}	6.0	$1.19 \times 10^{-2\,b,c}$
4.0×10^{-2}	3.1	4.9×10^b	4.3×10^{-4}	7.0	$1.24\ t\ 10^{-2\,b,c}$

[a] $\mu = 1.0$ M ($LiClO_4$); $T = 25.0$ °C; $[IrCl_6^{2-}]_0 = (0.5\text{–}1) \times 10^{-4}$ M. [b] $[Na_4P_2O_7] = 5.0 \times 10^{-4}$ M. [c] Used to obtain k_1 by eq 5.

Table II. Acid Dependence of $IrCl_6^{2-}$–HNO_2 Reactions below pH 2[a]

[N(III)], M	$[H^+]$, M	k_{obsd}, s^{-1} [b]	% completion[c]
4.0×10^{-2}	0.1	32	79
2.0×10^{-2}	0.1	16	92
4.0×10^{-3}	0.1	2.0	98
4.0×10^{-2}	0.25	9.7	60
4.0×10^{-2}	0.5	5.6	42
4.0×10^{-2}	1.0	2.8	33

[a] $\mu = 1.0$ M ($HClO_4$–$LiClO_4$); $T = 25.0$ °C; $[IrCl_6^{2-}]_0 = 5 \times 10^{-5}$ M. [b] k_{obsd} obtained from initial slopes of semilog plots. [c] Estimated uncertainty ±5.

range 2–5, this effect being more pronounced at higher [N(III)]; at higher pH the rates became pH independent. These results are presented in Table I. The results at high pH were analyzed according to eq 5. The second-order rate constant obtained by

$$-d[IrCl_6^{2-}]/dt = k_1[IrCl_6^{2-}][NO_2^-] \quad (5)$$

using the indicated data in Table I and eq 5 is $k_1 = (26.9 \pm 1.6)$ M^{-1} s^{-1}. This value for k_1 is slightly greater than previously obtained (19 M^{-1} s^{-1}),[12] as expected at this higher ionic strength for a reaction between ions of similar charge. At pH 2, the order with respect to [N(III)] was 1.46. Below pH 2 the rate constants decreased with acidity, and the reaction did not go to completion; a typical example of this behavior is shown in Figure 2. Under these conditions the semilog plots were distinctly nonlinear, and rate constants were obtained as the initial slopes of these plots. These data are reported in Table II. Attempted experiments to measure the rate of reaction of $IrCl_6^{2-}$ with nitric oxide in aqueous solution at pH 7 and 0 directly in the stopped flow were not successful because the reaction was complete within the dead time of the instrument.

$IrCl_6^{3-}$ Reactions. Between pH 0 and 1 the reaction of $IrCl_6^{3-}$ with N(III) did not go to completion, and for pH >1 there was no detectable reaction. The product spectrum corresponded to

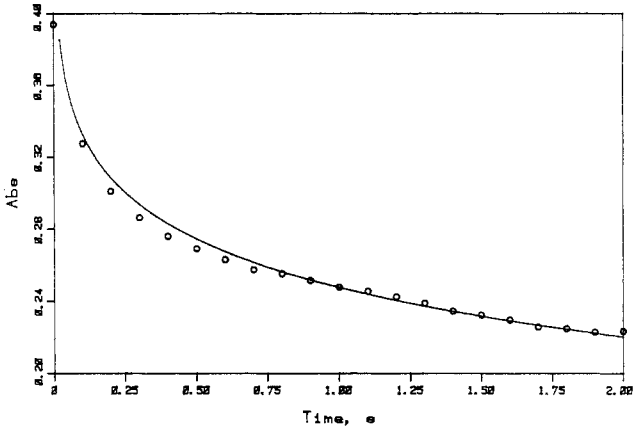

Figure 2. Product inhibition for reaction of $IrCl_6^{2-}$ with N(III) in strongly acidic media: 0.25 M $HClO_4$, 0.75 M $LiClO_4$, $[IrCl_6^{2-}]_0 = 1.1 \times 10^{-4}$ M, $[HNO_2] = 4.0 \times 10^{-2}$ M. Solid line is a simulation.

Table III. Kinetics Data for $IrCl_6^{3-}$–HNO_2 Reaction in Perchlorate Media[a]

$[HNO_2]$, M	$[H^+]$, M	k_f', s^{-1} [b]	A_∞ [c]	K_4, M	$10^{-4}k_{-4}$, M^{-2} s^{-1} [b]
1.0×10^{-3}	1.0	18	0.27 ± 0.07	64	1.8
2.0×10^{-3}	1.0	37	0.27 ± 0.07	133	1.9
5.0×10^{-4}	1.0	14	0.16 ± 0.05	94	2.8
1.0×10^{-3}	0.25	5.5	0.12 ± 0.04	84	2.2
2.0×10^{-3}	0.25	20	0.18 ± 0.05	74	4.1
2.0×10^{-3}	0.1	4.0	0.08 ± 0.04	150	2.0

[a] $\mu = 1.0$ M ($HClO_4$–$LiClO_4$); $T = 25.0$ °C, $[IrCl_6^{3-}]_0 = 3.0 \times 10^{-4}$ M. [b] Equation 8. [c] Final absorbance; used to calculate K_4.

that of $IrCl_6^{2-}$ with less than a 5% yield of $IrCl_5(H_2O)^-$ as determined from the ratio of the absorbances at 460 and 490 nm. The ratio for $IrCl_6^{2-}$ was 0.51, and that for $IrCl_5H_2O^-$ was 1.37 while the product of the reaction of $IrCl_6^{3-}$ (3.0×10^{-4} M) and HNO_2 (1.0×10^{-2} M) in 1.0 M $HClO_4$ (after oxidation with chlorine for complete conversion to Ir(IV)) had a ratio of 0.61; this divergence from a yield of pure $IrCl_6^{2-}$ corresponds to the known rate of spontaneous aquation of $IrCl_6^{3-}$.[2] However, there was no indication of the formation of the nitrosyl complex. The nitrosyl complex was particularly sought because of its reported preparation from identical reagents under slightly different conditions.[13]

As Fe(II) is reported to reduce NO to N_2O[14] and as NO is a strong oxidizing agent (1.59 V for the NO/N_2O couple in 1 M H^+),[15] we looked for N_2O in the products of the reaction of $IrCl_6^{3-}$ (1.0×10^{-3} M) and HNO_2 (1.0×10^{-2} M) in 1 M $HClO_4$. N_2O could not be detected as a product of the reaction; within the sensitivity of the method, its yield was less than 5×10^{-6} M.

In 1 M $HClO_4$, a mixture of NO (1.9×10^{-3} M) and $IrCl_6^{3-}$ (3×10^{-4} M) did not produce $IrCl_6^{2-}$ or any nitrosyl complex of Ir(IV),[13] as was apparent from the lack of development of any color in the solution. It was inferred that there was no reaction between $IrCl_6^{3-}$ and NO.

These observations are consistent with the reaction given in eq 6, which is presented in inverted notation so as to be consistent with our prior study of nitrous acid chemistry.[1] The equilibrium

$$IrCl_6^{3-} + HNO_2(aq) + H^+ \rightleftarrows IrCl_6^{2-} + NO(aq) + H_2O \quad k_{-4},\ k_4,\ K_4^{-1} \quad (6)$$

constant, K_4, for this reaction was calculated from the yield of $IrCl_6^{2-}$. Two such experiments were performed in the hand-stopped flow. With $[IrCl_6^{3-}]_0 = 4.5 \times 10^{-4}$ M, $[H^+] = 1.0$ M, $[HNO_2] = 1.0 \times 10^{-2}$ M, and no added nitric oxide, the final absorbance was 0.66 A; this leads to $K_4 = 111$ M. With $[IrCl_6^{3-}]$

(14) Bonner, F. T.; Pearsall, K. A. *Inorg. Chem.* **1982**, *21*, 1973.
(15) Bard, A. J., Ed. "Encyclopedia of Electrochemistry of the Elements"; Dekker: New York, 1978; Vol. 8, p 324.

Table IV. Zero-Order Rate Constants for the $IrCl_6^{3-}$ Reaction in Nitrate Media

$[HNO_2]$, M	$[H^+]$, M	$[NO_3^-]$, M	K_4,[b] M	k, M s^{-1}	k_{calcd},[c] M s^{-1}
1.0×10^{-3}	2.0	2.0	74	6.6×10^{-5}	5.9×10^{-5}
2.0×10^{-3}	2.0	2.0	88	1.1×10^{-4}	9.8×10^{-5}
4.0×10^{-3}	2.0	2.0	88	1.59×10^{-4}	1.47×10^{-4}
1.0×10^{-2}	2.0	2.0	100	2.66×10^{-4}	2.11×10^{-4}
1.0×10^{-3}	0.5	2.0	55	1.37×10^{-5}	1.46×10^{-5}
2.0×10^{-3}	0.5	2.0	99	2.7×10^{-5}	2.5×10^{-5}
4.0×10^{-3}	0.5	2.0	117	3.9×10^{-5}	3.7×10^{-5}
1.0×10^{-2}	0.5	2.0	89	6.8×10^{-5}	5.3×10^{-5}
1.0×10^{-3}	1.0	2.0	89	2.7×10^{-5}	2.9×10^{-5}
4.0×10^{-3}	1.0	2.0	165	4.4×10^{-5}	7.4×10^{-5}
1.0×10^{-2}	1.0	2.0	145	7.8×10^{-5}	1.06×10^{-5}
1.0×10^{-3}	2.0	0.5	46	1.7×10^{-5}	1.5×10^{-5}
1.0×10^{-3}	2.0	0.2	84	7.0×10^{-6}	5.9×10^{-6}

[a] μ = 2.0 M ($LiClO_4$); T = 25.0 °C; $[IrCl_6^{3-}]_0 = 1.5 \times 10^{-4}$ M. [b] K_4 calculated from the prompt yield of $IrCl_6^{2-}$, as determined by extrapolating the zero-order plots to t_0. The estimated uncertainty is at least ±20%, and it is related to the difficulty in obtaining precise absolute absorbance values on the stopped-flow instrument. [c] k_{calcd} obtained from nonlinear least-squares fit of eq 9.

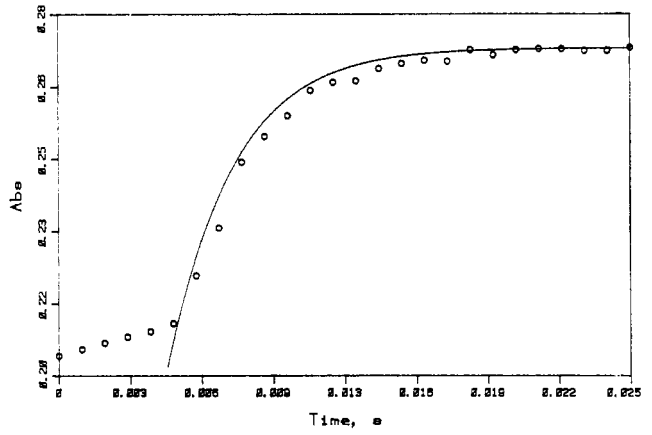

Figure 3. "Prompt" oxidation of $IrCl_6^{3-}$ by nitrous acid: 1.0 M $HClO_4$, $[IrCl_6^{3-}]_0 = 3.8 \times 10^{-4}$ M, $[HNO_2] = 2.0 \times 10^{-3}$ M. Solid line is a simulation with the time axis adjusted to allow for the delay between triggering and termination of the flow in the apparatus.

$= 4.0 \times 10^{-4}$ M, $[H^+]$ = 1.0 M, $[HNO_2] = 1.0 \times 10^{-2}$ M, and added nitric oxide at $[NO] = 9.5 \times 10^{-4}$ M, the final absorbance was 0.23 A, and so K_4 = 61 M. K_4 was also calculated from the final absorbance values in the kinetics studies of the "prompt" reactions reported in Tables III and IV. These results are randomly scattered between 55 and 150 M. The admittedly large scatter is tentatively attributed to the presence of small amounts of $IrCl_5(H_2O)^{2-}$ and to uncertainties in the initial absorbances; the collected data give $K_4 = 92 \pm 26$ M. This is in good agreement with K_4 = 64 as calculated from the $IrCl_6^{2-/3-}$ potential (E_f = 0.93 V at μ = 1.0 M ($HClO_4$)),[16,17] the $HNO_2/NO(g)$ potential ($E°$ = 0.984),[18,19] and the solubility of NO ($H = 1.9 \times 10^{-3}$ M atm^{-1}).[7]

Attempts to measure the kinetics for eq 6 were constrained by small absorbance changes and very rapid rates. No data could be obtained with added NO because at low $[HNO_2]$ the absorbance changes were too small and at higher $[HNO_2]$ the rates were too great. Complications arising from contamination by O_2 are described in the Experimental Section. The kinetics runs that could be obtained within these limitations occurred in 25–50 ms and were analyzed in terms of rate law 7. A typical example

$$d[IrCl_6^{2-}]/dt = k_{-4}[IrCl_6^{3-}][HNO_2][H^+] - k_4[NO][IrCl_6^{2-}] \quad (7)$$

(16) Kravtsov, V. I.; Petrova, G. M. *Russ. J. Inorg. Chem.* (*Engl. Transl.*) **1964**, *9*, 552.
(17) George, P.; Hanania, G. I. H.; Irvine, D. H. *J. Chem. Soc.* **1957**, 3048.
(18) Schmid, G.; Neumann, U. *Z. Phys. Chem.* **1967**, *54*, 150.
(19) Wagman, D. D.; et al. *NBS Tech. Note* (*U.S.*) **1968**, *No. 270–3*.

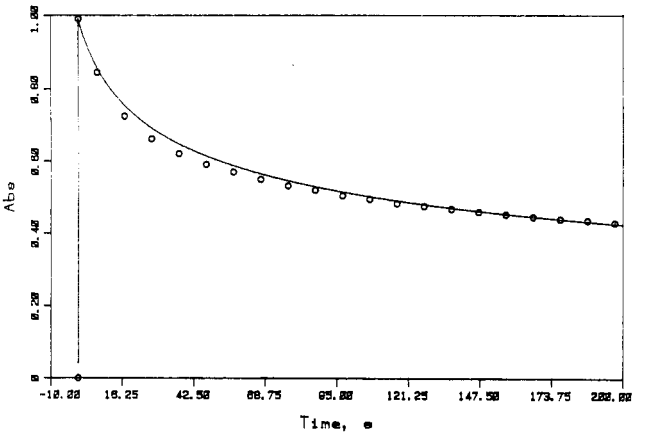

Figure 4. Biphasic reaction of $IrCl_6^{3-}$ at high [N(III)]: 1.0 M $HClO_4$, $[IrCl_6^{3-}]_0 = 5.5 \times 10^{-4}$ M, $[HNO_2] = 4.0 \times 10^{-2}$ M. Solid line is a simulation.

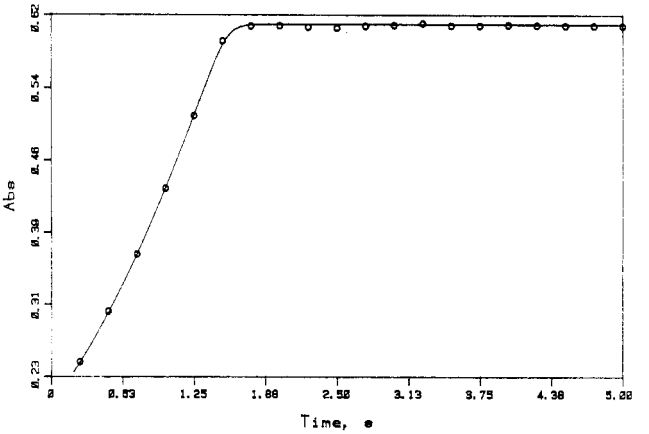

Figure 5. Zero-order reaction of $IrCl_6^{3-}$ in nitrous acid/nitric acid mixture: 2.0 M HNO_3, $[IrCl_6^{3-}]_0 = 1.53 \times 10^{-4}$ M, $[HNO_2] = 1.0 \times 10^{-3}$ M. Solid line is a simulation.

is shown in Figure 3. The integrated form of rate law 7 is eq 8, where $\alpha_0 = [IrCl_6^{2-}]_\infty$, and $k_f' = k_{-4}[HNO_3][H^+]$. These results

$$-\ln\left\{\frac{\alpha_0^2 + 2\alpha_0[IrCl_6^{3-}]_\infty}{\alpha_0 - A_t/\epsilon} - [IrCl_6^{3-}]_\infty\right\} = \ln(\alpha_0 - [IrCl_6^{3-}]_\infty) - \left(\frac{\alpha_0 + 2[IrCl_6^{3-}]_\infty}{\alpha_0}\right)k_f' t \quad (8)$$

are presented in Table III; they lead to $k_{-4} = (2.5 \pm 0.9) \times 10^4$ M^{-2} s^{-1}, and by the principle of detailed balancing, $k_4 = 2.3 \times 10^6$ M^{-1} s^{-1}. Although the data are not of sufficient quality to define rate law 7 unambiguously, we feel that the rate law does provide a concise description of the results.

As shown in Figure 4, at very high [N(III)] the $IrCl_6^{2-}$ formed in the rapid phase was found to be reduced again in a slower phase with non-first-order kinetics characteristic of product inhibition.

In nitrate media, the rapid initial reaction was followed by a slower reaction that reached near completion, and that was roughly zero order with respect to [Ir(III)]; a typical example is shown in Figure 5. The data are presented in Table IV and are approximately described by rate law 9 with $k_{-2} = (9.2 \pm 2.0) \times 10^{-3}$

$$\frac{d[IrCl_6^{2-}]}{dt} = \frac{2k_{-2}[H^+][NO_3^-][N(III)]}{1 + [N(III)]k'} \quad (9)$$

M^{-2} s^{-1} and $k' = (2.47 \pm 0.96) \times 10^2$ M^{-1}, although there are some systematic deviations. Reactions carried out with $IrCl_6^{3-}$ ((3–6) $\times 10^{-4}$ M) in excess over HNO_2 (2×10^{-5} M) in nitric acid media gave autocatalytic kinetics as shown in Figure 6.

$IrBr_6^{3-}$, $IrBr_5(H_2O)^{2-}$, and $IrCl_5(H_2O)^{2-}$. To understand the reaction of $IrCl_6^{3-}$ with HNO_2 better, we briefly looked at the

reaction of HNO_2 with $IrBr_6^{3-}$. In 1 M $HClO_4$ solution, with $[HNO_2] = 1.0 \times 10^{-3}$ M and $[IrBr_6^{3-}] = 1.0 \times 10^{-4}$ M, the reaction produced a 75% yield of $IrBr_6^{2-}$ with a pseudo-first-order rate constant of 90 s^{-1}. By thermodynamic arguments the reaction should have proceeded to completion ($E_f(IrBr_6^{2-/3-}) = 0.84$ V).[20] As the solutions aged, the yield of $IrCl_6^{2-}$ decreased and the apparent rate constants increased. These effects are apparently related to aquation of $IrBr_6^{3-}$. In analogy with the $IrCl_6^{3-}$ reaction with HNO_2, the $IrBr_6^{3-}$ reaction can be given by eq 10. Assuming

$$IrBr_6^{3-} + HNO_2 + H^+ \rightleftarrows IrBr_6^{2-} + NO + H_2O \quad k_{-4}', k_4' \tag{10}$$

rate law 11 for this reaction, the value of k_{-4}' is 9.0×10^4 M^{-2} s^{-1}, but this is probably an overestimate since even under the most favorable conditions some aquation had occurred. However, the reaction does have the advantage of larger absorbance changes and lower rates than the $IrCl_6^{3-}$ reaction.

$$d[IrBr_6^{2-}]/dt = k_{-4}'[IrBr_6^{3-}][HNO_2][H^+] \tag{11}$$

Oxidation of $IrCl_5(H_2O)^{2-}$ and $IrBr_5(H_2O)^{2-}$ by N(III) did not take place even at $[H^+] = 1$ M.

NO_2 + $[Fe(TMP)_3]^{2+}$. Pulse-radiolytic studies were performed on mixtures of 5×10^{-3} M $NaNO_2$ and $[Fe(TMP)_3]SO_4$ that were saturated with N_2O. Irradiation was accompanied by a prompt ($t_{1/2} < 10$ μs) minor rise in absorbance and a subsequent larger first-order absorbance increase. The absorbance increase in both cases is attributed to formation of $[Fe(TMP)_3]^{3+}$ ($\epsilon_{370} = 5460$ M^{-1} cm^{-1}, $\epsilon_{665} = 1560$ M^{-1} cm^{-1}). The yield of the prompt process increased with increasing $[Fe(TMP)_3^{2+}]$, but the yield in the slower process was independent of $[Fe(TMP)_3^{2+}]$; overall, the yield of $[Fe(TMP)_3]^{3+}$ was about two-thirds the yield of e^- and OH predicted from the dose. The pseudo-first-order rate constants and yields per dose for the second process were independent of irradiation dose or monitoring wavelength. Experiments carried out at $[Fe(TMP)_3^{2+}] = 5.0 \times 10^{-4}$ and 9.0×10^{-5} M demonstrated a first-order dependence on $[Fe(TMP)_3^{2+}]$ for the rate of the second process. If it is assumed that the reactive species is NO_2 (see eq 13–19 below), then these results lead to a rate constant of $(1.0 \pm 0.3) \times 10^7$ M^{-1} s^{-1} for the reaction

$$[Fe(TMP)_3]^{2+} + NO_2 \rightarrow [Fe(TMP)_3]^{3+} + NO_2^- \tag{12}$$

This assignment is based on the following mechanism:

$$H_2O \rightsquigarrow OH, e^-, H, \text{etc.} \tag{13}$$

$$e^- + N_2O \xrightarrow{H^+} N_2 + OH \quad 8.0 \times 10^9 M^{-1} s^{-1}\ ^{21} \tag{14}$$

$$OH + NO_2^- \rightarrow OH^- + NO_2 \quad 5.0 \times 10^9\ M^{-1} s^{-1}\ ^{22} \tag{15}$$

$$e^- + NO_2^- \rightarrow NO_2^{2-} \quad 8.1 \times 10^9\ M^{-1} s^{-1}\ ^{21} \tag{16}$$

$$NO_2^{2-} \xrightarrow{H^+} NO + H_2O \quad 6 \times 10^4\ s^{-1}\ ^{23} \tag{17}$$

$$NO + NO_2 \rightarrow N_2O_3 \quad 1.1 \times 10^9\ M^{-1} s^{-1}\ ^{24} \tag{18}$$

$$NO_2^{2-} + NO_2 \rightarrow 2NO_2^- \quad \text{(fast?)} \tag{19}$$

$$[Fe(TMP)_3]^{2+} + OH \rightarrow [Fe(TMP)_3]^{3+} + OH^- \tag{20}$$

The prompt absorbance rise is attributed to competition for OH by NO_2^- and $[Fe(TMP)_3]^{2+}$. The well-documented formation of NO_2^{2-}[23] and its subsequent reactions divert about one-third of the initial OH + e^- from formation of NO_2; therefore, the yield of $[Fe(TMP)_3]^{3+}$ is expected to be only two-thirds that of the initial OH + e^-, and this expectations was verified in the experiments. Possible complications include the formation of N_2O_4 from NO_2 ($K = 6.5 \times 10^4$ M^{-1})[23] and the second-order hydrolysis of NO_2. The observations that the second process was pseudo first order and that the yields and rate constants were independent of dose indicate that these complications were not significant. Numerical simulations (vide infra) have also confirmed that these complications were not significant at the radical concentrations of these studies ($[NO_2]_0 \sim 4 \times 10^{-6}$ M).

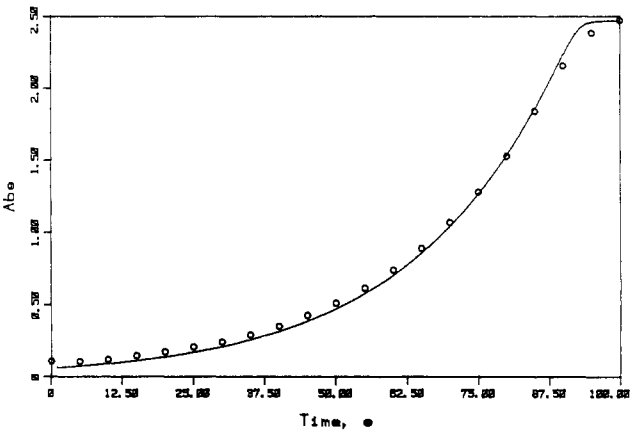

Figure 6. Autocatalytic oxidation of $IrCl_6^{3-}$ by nitric acid: 2.0 M HNO_3, $[IrCl_6^{3-}]_0 = 6.18 \times 10^{-4}$ M, $[HNO_2] = 2.0 \times 10^{-5}$ M. Solid line is a simulation.

Table V. Rate Constants Used in Numerical Simulations

k_{-3}, M^{-1} s^{-1}	1.75×10^8 (our simulations)
k_{-4}, M^{-1} s^{-1}	1.8×10^4 (our results, Table III)
k_2, M^{-1} s^{-1}	5.0×10^7 (ref 26)
k_{-2}, M^{-1} s^{-1}	1.22×10^{-2} (our simulations)

reaction type	k_3, M^{-1} s^{-1}	$10^{-6}k_4$, M^{-1} s^{-1}
"normal" (Figure 1)	25	2.5
product inhibition (Figure 2)	10	1.15
"prompt" (Figure 3)	12	2.5
biphasic (Figure 4)	12	3.6
zero order (Figure 5)	12	1.4
autocatalytic (Figure 6)	12	1.4
oxygen effect (Figure 7)	12	1.6

Numerical Simulations

Simulations of the hexachloroiridate(III,IV) reactions with nitrous acid were obtained by numerical integration[25] of the differential equations arising from the mechanism in Scheme I.

Scheme I

$$2HNO_2 \rightleftarrows NO + NO_2 + H_2O \quad k_3, k_{-3}, K_3 \tag{21}$$

$$H_2O + 2NO_2 \rightleftarrows NO_3^- + HNO_2 + H^+ \quad k_2, k_{-2}, K_2 \tag{22}$$

$$H_2O + IrCl_6^{2-} + NO \rightleftarrows IrCl_6^{3-} + HNO_2 + H^+ \quad k_4, k_{-4}, K_4 \tag{23}$$

Scheme I appears to describe the $IrCl_6^{2-}/IrCl_6^{3-}$ system in nitrous acid adequately, as can be seen from simulations of six different kinetic patterns (Figures 1–6). Rate constants used in

(20) Stanbury, D. M.; Wilmarth, W. K.; Khalaf, S.; Po, H. N.; Byrd, J. E. *Inorg. Chem.* **1980**, *19*, 2715.
(21) Ross, A. B. *Natl. Stand. Ref. Data Ser. (U.S. Natl. Bur. Stand.)* **1975**, *NSRDS-NBS 43*, Supplement.
(22) Farhataziz; Ross, A. B. *Natl. Stand. Ref. Data Ser. (U.S. Natl. Bur. Stand.)* **1977**, *NSRDS-NBS* 59.
(23) Gratzel, M.; Henglein, A.; Lilie, J.; Beck, G. *Ber. Bunsenges. Phys. Chem.* **1969**, *73*, 646.
(24) Gratzel, M.; Taniguchi, S.; Henglein, A. *Ber. Bunsenges. Phys. Chem.* **1970**, *74*, 488.

(25) Integrations were performed on a DEC 11/70 minicomputer and on a 128K Macintosh personal computer by using Hindmarsh and Byrne's subroutine EPISODE. EPISODE is efficient in solving stiff systems of differential equations, requiring only 5 s on the DEC 11/70 to solve the typical systems in this paper; on the Macintosh, integrations typically took 50 s. EPISODE supplies several methods for integration; although they were found to vary in efficiency, they yielded virtually identical solutions. Nonlinear least-squares fitting to the data was performed with the Los Alamos nonlinear least-squares program on the same computers; the data were weighted as $1/k_{obsd}$.

the simulations are presented in Table V.

The "Prompt" Reactions (Figure 3). The "prompt" reactions were the reactions of $IrCl_6^{3-}$ with N(III) in acidic media, where the equilibrium in eq 6 was rapidly established. The simulations of these reactions were sensitive only to the rate constants k_4 and k_{-4}; a best fit was obtained by using rate constants quite similar to those obtained in the analytical fit to eq 8. These results serve as a simple test of the method, and they demonstrate that the various equilibria in nitrous acid do not invalidate the analytical treatment in eq 8.

The Zero-Order Reactions (Figure 5). Simulations of the zero-order reactions (in nitrate media) were found to be sensitive to the ratios k_4/k_{-4} and k_3/k_{-3}, but they were insensitive to the values of the individual rate constants k_4, k_{-4}, k_3, and k_{-3}. Thus, equilibria K_4 and K_3 are rapid on the time scale of the experiments. These two equilibria control the initial absorbance and the qualitative shape of the curves; note how the slight upward curvature in Figure 5 is correctly simulated. Rate constants k_2 and k_{-2} affect the overall rate of the reactions and the final absorbance. The simulation in Figure 5 was obtained with k_2 at its reported value,[26] k_{-4} at the value obtained from the "prompt" reactions, and k_3 at about the value reported by Stedman;[33] values for k_{-2}, k_4, and k_{-3} were then manually adjusted to obtain a good fit. The value of k_{-3} so obtained was retained for all the other simulations in this paper. By simulation of the experiments in 2 M H^+ at [N(III)] = (1, 4, and 10) $\times 10^{-3}$ M, the experimentally observed kinetic saturation with respect to [N(III)] was verified.

The net reaction under these conditions can be given by eq 24.

$$2IrCl_6^{3-} + NO_3^- + 3H^+ \rightleftarrows 2IrCl_6^{2-} + HNO_2 + H_2O \quad K_{24} \tag{24}$$

The position of this equilibrium can be calculated by using the various rate constants used in the simulation. In 2.0 M HNO_3, the reaction reaches completion at $[HNO_2] = 1.0 \times 10^{-3}$ M, but at $[HNO_2] = 1.0 \times 10^{-2}$ M, the reaction attains only 90% completion. The simulations match these results.

From our simulations, rate constant k_{-2} was found to be 1.2×10^{-2} M^{-2} s^{-1}. This value is in good agreement with the literature value 1.7×10^{-2} M^{-2} s^{-1},[27] measured by a similar zero-order reaction with thiocyanic acid.

The Autocatalytic Reactions (Figure 6). The reactions between $IrCl_6^{3-}$ and HNO_2 in nitric acid when $IrCl_6^{3-}$ is in excess over HNO_2 give autocatalytic kinetics. The reactions could be simulated with the same set of rate constants except for k_{-2}, whose value was adjusted to 9.2×10^{-3} M^{-1} s^{-1}. These simulations were also sensitive to the choice of K_3. For a fixed value of K_4, adjustments in k_4 and k_{-4} had no effect. The simulations clearly showed an accumulation of HNO_2 during the reaction, thus demonstrating that HNO_2 is the catalytic species.

The Biphasic Kinetics (Figure 4). At high $[HNO_2]$ in perchlorate media, the "prompt" oxidation of $IrCl_6^{3-}$ was followed by a slower reduction of $IrCl_6^{2-}$ that was formed. The simulations were sensitive to K_4, but when K_4 was held constant, the simulations of the second phase were not affected by changes in k_4 and k_{-4}. k_3 and k_4 were correlated in the sense that an increase in one could be compensated for by a decrease in the other, but k_{-2} had only a weak effect.

The Product Inhibition Kinetics (Figure 2). In perchlorate media, the reaction of $IrCl_6^{2-}$ with HNO_2 is non first order at $[H^+] > 0.1$ M, and it does not proceed to completion. The sensitivity of the simulations to changes in various rate constants was the same as in the biphasic kinetics.

The "Normal" Reactions (Figure 1). In contrast to the complex systems described above, the reactions of $IrCl_6^{2-}$ with HNO_2 in perchlorate media at pH >1.5 appeared "normal". The reactions reached completion and exhibited pseudo-first-order kinetics. The simulations were done on reactions at pH 2.0, where the reactions were fastest. The simulations were very sensitive to k_4 but were insensitive to k_{-4} and k_{-2}. They were also sensitive to K_3 and, for a given value of K_3, to the individual rate constants k_3 and k_{-3}.

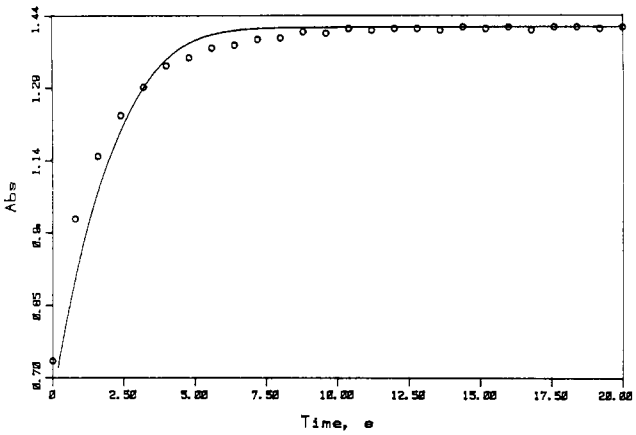

Figure 7. Oxygen effect on oxidation of $IrCl_6^{3-}$ by N(III): 1.0 M $HClO_4$, $[IrCl_6^{3-}]_0 = 4.0 \times 10^{-4}$ M, $[O_2] = 1.1 \times 10^{-3}$ M, $[HNO_2] = 1.0 \times 10^{-2}$ M. Solid line is a simulation.

The Oxygen Effect (Figure 7). In the early experiments on the oxidation of $IrCl_6^{3-}$ with HNO_2, it was found that the presence of oxygen shifted the position of eq 6 by a slower process. This was attributed to the removal of NO by reaction with oxygen. A typical example of this behavior is presented in Figure 7 for a solution saturated with oxygen. The slow shift of eq 6 by oxygen was simulated by including eq 25 in the numerical integrations.

$$NO + O_2 \rightarrow \text{products} \quad k_{25} \tag{25}$$

We have assumed this reaction to be first order in both NO and O_2 with a rate constant of 6.5×10^2 M^{-1} s^{-1}. In the gas phase the reaction is second order in NO, and it is believed to involve rate-limiting attack of NO on NO_3.[28] In solution, NO_3 has been reported to react with NO_2^- with $k = 1.2 \times 10^9$ M^{-1} s^{-1},[29] and so, under our conditions, formation of NO_3 may be rate limiting. These conclusions are tentative since only a very limited range of experiments were performed; they are presented primarily to demonstrate that the $IrCl_6^{2-/3-}$ couple can be used as a spectrophotometric indicator for the progress of the NO/O_2 reaction, a reaction that is otherwise difficult to observe.[30]

Discussion

The $IrCl_6^{2-/3-}$ couple displays a rich variety of kinetics phenomena in anaerobic solutions of nitrous acid, as demonstrated in Figures 1–6. These observations have been interpreted in terms of Scheme I by means of numerical integration. Scheme I consists of three reversible reactions, two of which describe the decomposition of nitrous acid and are well established; the third is the oxidation of NO to HNO_2 by $IrCl_6^{2-}$. Despite the alluring simplicity of Scheme I, it remains to be demonstrated that it is the best interpretation. The differences between Scheme I and the mechanism for the comparable $[Fe(TMP)_3]^{2+/3+}$ system invite careful scrutiny.

As in the prior study of the $[Fe(TMP)_3]^{2+/3+}$ reactions,[1] the thermochemistry of the nitrogenous species is a matter of some concern. The data in two NBS publications[19,31] differ with regard to $\Delta G_f°$ of NO_2^- and HNO_2, the revision deriving from a recalculation of data pertaining to the solubility of $AgNO_2$.[32] However, direct measurement of the NO/HNO_2 redox potential supports the earlier data.[18] In our simulations of the $IrCl_6^{2-/3-}$ system, consistent results could only be obtained with the older

(26) Lee, Y. N.; Schwartz, S. E. *J. Phys. Chem.* **1981**, *85*, 840.
(27) Hughes, M. N.; Phillips, E. D.; Stedman, G.; Whincup, P. A. E. *J. Chem. Soc. A* **1969**, 1148.
(28) Bamford, C. H.; Tipper, C. F. H. "Comprehensive Chemical Kinetics"; Elsevier, New York, 1972; Vol. VI, pp 169–172.
(29) Daniels, M. *J. Phys. Chem.* **1969**, *73*, 3710.
(30) Pogrebnaya, V. L.; Usov, A. P.; Baranov, A. V. *Appl. Chem. USSR (Engl. Transl.)* **1976**, *49*, 757.
(31) Wagman, D. D.; et al. *J. Phys. Chem. Ref. Data, Suppl.* **1982**, *11*, No. 2.
(32) Garvin, D., NBS, personal communication, 1984.

data. Our current pulse-radiolytic measurement of the rate of reduction of NO_2 by $[Fe(TMP)_3]^{2+}$, in conjunction with the rate of oxidation of NO_2^- by $[Fe(TMP)_3]^{3+}$, gives for reaction 1 an equilibrium constant of 2.6×10^3 and hence $E_f = 1.04$ V (μ = 0.3 M) for the NO_2/NO_2^- couple. This potential also supports the older data; we conclude that the older data are more correct, although there are still difficulties in accommodating Gratzel's data on N_2O_3.[24,33] Table VI compares equilibrium constants obtained from various sources.

Ir(IV) Reactions. At pH values greater than the pK_a of HNO_2, $IrCl_6^{2-}$ reacts directly with NO_2^-, as discussed in the earlier work.[12] The rate increase with increasing acidity on this reaction was quite surprising, and it stands in contrast with the reactions of $[Fe(bpy)_3]^{3+}$ and $[Fe(TMP)_3]^{3+}$ with N(III), where acid was found to inhibit the rates.[1,12] This rate increase could not be attributed to electrostatics. For example, hexachloroiridate(IV), although carrying a double negative charge, reacts with N_2H_4[4] and N_3^-[34] several orders of magnitude faster than with their protonated forms. Also, the order with respect to HNO_2 was 1.46, and a plot of $k_{obsd}/[HNO_2]$ vs. $[HNO_2]$ was not linear. This seems to rule out reduction by both HNO_2 and N_2O_3. NO_2 and N_2O_4 are unlikely reducing agents at such low acidities as pH 2 and 3.[35] The direct reaction of NO at 9×10^{-4} M with $IrCl_6^{2-}$ was too rapid for measurement; it is therefore likely that NO is the reactive species in N(III) solutions.

By applying a steady-state approximation for [NO] and $[NO_2]$, neglecting the reaction of $IrCl_6^{3-}$ with HNO_2 ($IrCl_6^{3-}$ was found not to become oxidized at these acidities), and approximating that $k_4[IrCl_6^{2-}] \ll k_{-3}[NO_2]$, we derived rate law 26 (see Appendix).

$$-d[IrCl_6^{2-}]/dt = (2k_2)^{1/3}(k_4K_3[IrCl_6^{2-}])^{2/3}[HNO_2]^{4/3} \quad (26)$$

The approximation that $k_4[IrCl_6^{2-}] \ll k_{-3}[NO_2]$ is probably not very precise, and the deviation of the experimental order with respect to $[HNO_2]$ of 1.46 may well reflect the severity of the approximation. Numerical simulations with Scheme I confirm the deviations from $^4/_3$ order and show that this ideal is approached at high concentrations of HNO_2. This rate law also implies that semilog plots of individual kinetics runs should be curved; slight curvature was observed. Integration of rate law 26 suggests that a plot of $[IrCl_6^{2-}]^{1/3}$ vs. time would be appropriate. Curvature was also found in these plots, and so the effective order lies between $^2/_3$ and 1. The experiment at pH 2 with $[HNO_2] = 4 \times 10^{-2}$ M (where rate law 26 should be most accurate) gave a value of 157 for $(k_4K_3)^{2/3}(2k_2)^{1/3}$. With values for k_2 and K_3 as in Tables V and VI, it is found that $k_4 = 1.8 \times 10^6$ M^{-1} s^{-1}. Numerical simulations including the same reactions gave best results for $k_4 = 1.5 \times 10^6$ M^{-1} s^{-1}, which serves to support the analysis.

Below pH 2 the rates showed an inverse-[acid] dependence and failed to reach completion; these observations simply reflect the reversibility of K_4.

Ir(III) Reactions. Unlike the reaction of $[Fe(TMP)_3]^{2+}$ with N(III), the reaction of $IrCl_6^{3-}$ with N(III) in perchlorate media could not be driven to completion at any acidity in the absence of NO_3^-. The reaction usually attained an equilibrium that was well in favor of the reactants under conditions where the kinetics of the reaction could be followed; when driven to completion in nitric acid media, it did so by a process zero order in $[IrCl_6^{3-}]$.

Kinetics data obtained in perchlorate media were treated by assuming reversible kinetics as in reaction 6. The value of k_{-4} thus obtained is $(2.5 \pm 0.9) \times 10^4$ M^{-2} s^{-1}, and the corresponding value for k_4 is 1.4×10^6 M^{-1} s^{-1}. This result compares quite favorably with that obtained from the reaction of $IrCl_6^{2-}$ with N(III) at pH 2 ($k_4 = (1.5\text{–}1.8) \times 10^6$ M^{-1} s^{-1}).

A lower limit for k_4 can be estimated from the direct reaction of NO with $IrCl_6^{2-}$. Since the reactions of $IrCl_6^{2-}$ with excess NO (9.5×10^{-4} M) in the pH range 0–7 went to completion within the dead time of the stopped-flow instrument, the half-life of the reaction must be $\ll$5 ms. This leads to $k_4 > 1.3 \times 10^5$ M^{-1} s^{-1}, which is consistent with the above treatments.

In nitrate media, NO_2 is produced by the reverse reaction in eq 22. The NO_2 produced subsequently reacts with NO in a rapid step by the reverse of reaction 21. As nitric oxide is thus consumed, reaction 23 is driven to the left by rapid reaction of $IrCl_6^{3-}$ with N(III). From a numerical integration of Scheme I including the six rate constants, the optimized value of k_{-2} was obtained as 1.2×10^{-2} M^{-2} s^{-1}. This value is in good agreement with a value obtained from a similar zero-order reaction of HNO_2 with thiocyanic acid (HSCN) in nitrate medium (1.7×10^{-2} M^{-2} s^{-1}).[33] This also leads to a value of 4.1×10^9 M for the equilibrium constant K_2, which is in good agreement with the older thermodynamic data[19] (see Table VI).

The net reaction in nitric acid medium is given in eq 24. The value of the equilibrium constant K_{24} can be calculated by using the $IrCl_6^{3-/2-}$ and HNO_3/HNO_2 potentials. Both of these may be assumed to be 0.94 V in μ = 2.0 M (HNO_3).[16,17,36] These potentials lead to $K_{24} = 1.0$ M^{-3}. From Scheme I, $K_{24} = K_3^2/K_4^2K_2$; from the rate constants in Table V, $K_{24} = 0.57$ M^{-3}, which is in good agreement with the thermochemical value. It can be seen from K_{24} that the zero-order reactions should not go to completion for $[N(III)] > 1.0 \times 10^{-3}$ M, which is consistent with the observations.

An analytical rate law for the zero-order reactions can be derived from Scheme I under the approximations that the reaction of NO_3^- with HNO_2 is irreversible and that equilibria denoted by K_3 and K_4 are attained rapidly. The rate law so derived is

$$\frac{d[IrCl_6^{2-}]}{dt} = \frac{2k_{-2}[NO_3^-][H^+][HNO_2]}{1 + [HNO_2][Ir]_{tot}\left(\frac{K_3K_4}{[H^+][IrCl_6^{3-}]^2} + \frac{[H^+]}{K_4[IrCl_6^{2-}]^2}\right)} \quad (27)$$

To the degree that the two terms on the right-hand side of the denominator compensate for each other, the denominator will be a constant, and thus the kinetics will be zero order in $[IrCl_6^{2-}]$. With this simplification it is clear that parameter k_{-2} in eq 9 is correctly identified and that k' in eq 9 is given by

$$k' = [Ir]_{tot}\left(\frac{K_3K_4}{[H^+][IrCl_6^{3-}]^2} + \frac{[H^+]}{K_4[IrCl_6^{2-}]^2}\right) \quad (28)$$

The above approximations are rather severe, and so the systematic deviations in the nonlinear least-squares fit are not unexpected. Nevertheless, the agreement among k_{-2} values obtained in this way, in the numerical integrations, and in the HSCN study is gratifying.

$IrCl_6^{2-/3-}$ vs. $[Fe(TMP)_3]^{2+/3+}$. With the mechanism for the $IrCl_6^{2-/3-}$ system established, meaningful comparisons with the $[Fe(TMP)_3]^{2+/3+}$ system can be made. It has already been pointed out that the oxidation of NO_2^- by $[Fe(TMP)_3]^{3+}$ is unusual in displaying product inhibition.[1] This is simply a consequence of the rate of the back-reaction of NO_2, which is almost 4 orders of magnitude greater than for the comparable $IrCl_6^{2-}$ reaction, as predicted by Marcus theory. In acidic media, comparison of the two systems is not as trivial.

For $[Fe(TMP)_3]^{3+}$, the acid dependence is such that there is a direct dependence on $[NO_2^-]$, and protonation inhibits the rates. In the $IrCl_6^{2-}$ system the rates increase with increasing acidity up to pH 2. Nitric oxide is produced in the self-decomposition of nitrous acid, and the rate of reaction of NO with $IrCl_6^{2-}$ ($k_4 = 1.0 \times 10^6$ M^{-1} s^{-1}) is far greater than the rate of reaction of NO_2^- ($k_1 = 3.0 \times 10^1$ M^{-1} s^{-1}). Hence, the rates increase with acidity. In the case of $[Fe(TMP)_3]^{3+}$, the nitrite reaction rate ($k_1 = 3.9 \times 10^3$ M^{-1} s^{-1}) is greater than the nitric oxide reaction rate ($k_4 < 1.0 \times 10^3$ M^{-1} s^{-1}), which leads to acid inhibition. The reactions proceed to a greater extent below pH 2 for $IrCl_6^{2-}$ than for $[Fe(TMP)_3]^{3+}$ because $IrCl_6^{2-}$ is the stronger oxidant.

(33) Stedman, G. *Adv. Inorg. Chem. Radiochem.* **1978**, *22*, 143.
(34) Ram, M. S.; Stanbury, D. M., unpublished work.
(35) Reference 15, p 448.
(36) Reference 15, p 325.

Table VI. Comparison of Equilibrium Constants with Literature Thermodynamic and Kinetic Data

	K_3, M	K_2, M	K_4,[a] M
$IrCl_6^{2-/3-}$–HNO_2 simulations	1.4×10^{-7}	4.1×10^{9}	78.0
older thermodynamic data[19]	1.1×10^{-7}	9.7×10^{9}	74.0
other kinetic results[36]	5.5×10^{-7}	7.7×10^{9}	
recent thermodynamic data[31]	6.0×10^{-6}	4.6×10^{8}	8.6

[a] Obtained by using 0.93 V as the $IrCl_6^{2-/3-}$ potential, with μ = 1.0–2.0 M.[16,17]

With $[Fe(TMP)_3]^{2+}$, the reaction with nitrous acid reaches completion in the acidity range $[H^+]$ = 0.1–1.0 M. With $IrCl_6^{3-}$, the reaction reaches only an equilibrium position. In both cases the stoichiometry indicates reduction of nitrous acid to nitric oxide, and the degree of completion reflects the relative reduction potentials of $IrCl_6^{3-}$ and $[Fe(TMP)_3]^{2+}$.

Added nitric oxide suppresses the rate of reaction of $[Fe(TMP)_3]^{2+}$ with N(III), but there is no acid dependence. The oxidizing species is NO_2, whose concentration in nitrous acid is lowered by added nitric oxide. In the case of $IrCl_6^{3-}$ the rates are unaffected by added nitric oxide but are first order in acid. This mechanistic crossover results from two opposing trends. The NO_2 pathway (k_{-1}) is $\approx 10^4$-fold faster for $[Fe(TMP)_3]^{2+}$ than for $IrCl_6^{3-}$ as predicted by Marcus theory.[1] On the other hand, the k_{-4} pathway is at least 100-fold faster for $IrCl_6^{3-}$ than for $[Fe(TMP)_3]^{2+}$, and this can be explained in terms of the differing electrostatics.

Intimate Mechanism. Rate laws having terms first order in substrate, acidity, and HNO_2 are generally interpreted according to the two-step process

$$HNO_2 + H^+ \rightleftarrows H_2O + NO^+ \quad K_5 \qquad (29)$$

$$NO^+ + \text{substrate} \rightarrow \text{products} \quad k'' \qquad (30)$$

where the third-order rate constant, k_{-4}, equals K_5k''.[37] Equilibrium K_5, as discussed in Stedman's review, is attained rapidly,[33] and the step should be rate limiting only for $[IrCl_6^{3-}] > 3 \times 10^{-2}$ M. The exact value of K_5 is a matter of some dispute, but the most reliable value appears to be 3×10^{-7} M^{-1}.[37] In the case of the $IrCl_6^{3-}$ reaction, k'' refers to the process

$$NO^+ + IrCl_6^{3-} \rightarrow NO + IrCl_6^{2-} \quad k'' \qquad (31)$$

Thus for the reaction of $IrCl_6^{3-}$ we have $k'' = 7 \times 10^{10}$ M^{-1} s^{-1}, which is at the diffusion-controlled limit for a reaction of this charge type. Stedman et al. have calculated a value of 3.2×10^4 M^{-2} s^{-1} for the third-order rate constant, K_5k'', for reactions of this charge type having the k'' step diffusion controlled,[38] and this is quite comparable with our value of 1.8×10^4 M^{-2} s^{-1} for k_{-4}. Diffusion-controlled reactions of NO^+ appear to be fairly common.[33,37]

The NO/NO^+ reaction proceeds without substitution at $IrCl_6^{2-/3-}$; however, it is difficult to define the coordination sphere for NO/NO^+. The concept of outer sphere vs. inner sphere is thus difficult to apply, and the concept of strong overlap vs. weak overlap is more appropriate in this context. If the reaction is a case of weak overlap, then it may be anticipated that it can be described in terms of Marcus/Hush theory. By using a classical valence force-field model, Eberson and Radner have calculated that the NO^+/NO and NO_2/NO_2^- self-exchange reactions should have equal rate constants of $\sim 1 \times 10^{-2}$ M^{-1} s^{-1}.[39] Previous studies have supported this estimate in the case of the NO_2/NO_2^- couple.[1,3] Applying the Marcus/Hush cross relationship to the current data in the usual way[3] leads to an estimate of 4×10^8 M^{-1} s^{-1} for the self-exchange rate constant for the NO^+/NO redox couple. Little numerical significance should be attributed to this calculation, but it emphasizes that the reaction of NO^+ with $IrCl_6^{3-}$ has virtually no barrier. If the cross relationship is used to predict the rate constant for the reaction of NO^+ with $IrCl_6^{3-}$, a value of 4×10^5 M^{-1} s^{-1} is obtained, rather than the diffusion-controlled rate that was observed. This is a substantial discrepancy. Although it is tempting to attribute the observed enhancement in rate to nuclear tunneling, a plausible alternative explanation would be strong overlap. Strong overlap could be envisioned as occuring with NOCl coordinated to Ir(IV) as an intermediate. Inner-sphere reactions of $IrCl_6^{2-}$ have been demonstrated for reduction by Cr^{2+},[40] and strong overlap has been inferred for reductions by various metal alkyls.[41]

Conclusions. An enormous variety of kinetics phenomena can occur with the $IrCl_6^{2-/3-}$ system in nitrous acid. These have been quantitatively described in terms of the reversible reaction of $IrCl_6^{3-}$ with NO^+ to form $IrCl_6^{2-}$ + NO, along with a number of established reactions between the various nitrogenous species. The diffusion-controlled attack of NO^+ on $IrCl_6^{3-}$ vastly exceeds the rate predicted by Marcus/Hush theory and may be rationalized as due to nuclear tunneling or to strong overlap.

Acknowledgment. This research was supported by the National Science Foundation (Grant CHE-8215501) and by the Robert A. Welch Foundation. The experiments and analyses of the data produced in the pulse-radiolysis experiments were performed with the assistance of Steve Atherton at the Center for Fast Kinetics Research at the University of Texas at Austin. The CFKR is supported jointly by the Biotechnology Branch of the Division of Research Resources of NIH (Grant RR00886) and by the University of Texas at Austin. We are grateful for the helpful comments of David Garwin (NBS), David Ross (SRI International), and Stephen Schwartz (Brookhaven).

Appendix

Derivation of Eq 26. Equation 26 is derived from eq 21, 22, and 23 with neglect of k_{-4} as follows:

$$-d[IrCl_6^{2-}]/dt = k_4[NO][IrCl_6^{2-}] \qquad (A1)$$

Steady-state approximations are applied to [NO] and $[NO_2]$ to give

$$(d[NO]/dt)_{ss} = 0 = k_3[HNO_2]^2 - k_{-3}[NO]_{ss}[NO_2]_{ss} - k_4[NO]_{ss}[IrCl_6^{2-}] \qquad (A2)$$

$$[NO]_{ss} = k_3[HNO_2]^2/(k_{-3}[NO_2]_{ss} + k_4[IrCl_6^{2-}]) \qquad (A3)$$

$$(-d[NO_2]/dt)_{ss} = 0 = k_3[HNO_2]^2 - k_{-3}[NO]_{ss}[NO_2]_{ss} - 2k_2[NO_2]_{ss}^2 \qquad (A4)$$

Substituting eq A3 into eq A4 and rearranging yield

$$0 = k_3k_4[HNO_2]^2[IrCl_6^{2-}] - 2k_2[NO_2]_{ss}^2(k_4[IrCl_6^{2-}] + k_{-3}[NO_2]_{ss}) \qquad (A5)$$

Under the approximation that $k_4[IrCl_6^{2-}] << k_{-3}[NO_2]_{ss}$, eq A5 leads to

$$[NO_2]_{ss} = (k_3k_4/2k_2k_{-3})[HNO_2]^2[IrCl_6^{2-}]^{1/3} \qquad (A6)$$

By application of the same approximation to eq A3 and substitution of eq A6 into eq A3, the steady-state concentration of NO can be derived; i.e.

$$[NO]_{ss} = (2k_2/k_4)^{1/3}(k_3/k_{-3})^{2/3}[HNO_2]^{4/3}/[IrCl_6^{2-}]^{1/3} \qquad (A7)$$

Substitution of eq A7 into eq A1 leads to the rate law

$$-d[IrCl_6^{2-}]/dt = (2k_2)^{1/3}(k_4K_3[IrCl_6^{2-}])^{2/3}[HNO_2]^{4/3} \qquad (A8)$$

Derivation of Eq 27. Equation 27 may be derived by first making the approximations that the equilibria denoted by K_3 and K_4 are established rapidly on the time scale of the experiment. If an increment x of NO_2 is introduced, reequilibration by K_3 will

(37) Ridd, J. H. *Adv. Phys. Org. Chem.* **1978**, *16*, 1.
(38) Bates, J. C.; Reveco, P.; Stedman, G. *J. Chem. Soc., Dalton Trans.* **1980**, 1487.
(39) Eberson, L.; Radner, F. *Acta Chem. Scand., Ser. B* **1984**, *38*, 861.
(40) Sykes, A. G.; Thorneley, R. N. F. *J. Chem. Soc. A* **1970**, 232.
(41) Fukuzumi, S.; Wong, C. L.; Kochi, J. K. *J. Am. Chem. Soc.* **1980**, *102*, 2928.

reduce [NO] and [NO_2] by a decrement y; the corresponding increment to [HNO_2] is neglected, although numerical simulations show that [HNO_2] actually increases by ~10% during the reaction. Reequilibration by K_4 reduces [$IrCl_6^{3-}$] by z (the corresponding decrements to [H^+] and [HNO_2] also being neglected) and increases [NO] and [$IrCl_6^{2-}$] by z. The resulting equilibria are given as

$$K_3 = \frac{([NO]_0 - y + z)([NO_2]_0 - y + x)}{[HNO_2]^2} \quad \text{(A9)}$$

$$K_4 = \frac{([IrCl_6^{3-}]_0 - z)[H^+][HNO_2]}{([IrCl_6^{2-}]_0 + z)([NO]_0 - y + z)} \quad \text{(A10)}$$

Solving eq A10 for y yields

$$y = [NO]_0 - \frac{([IrCl_6^{3-}]_0 - z)[H^+][HNO_2]}{([IrCl_6^{2-}]_0 + z)K_4} + z \quad \text{(A11)}$$

Inserting this expression for y into eq A9 (with the definition $[Ir]_{tot} = [IrCl_6^{2-}]_0 + [IrCl_6^{3-}]_0$) and solving for x yield

$$x = \frac{K_3K_4[HNO_2][IrCl_6^{2-}]}{([Ir]_{tot} - [IrCl_6^{2-}])[H^+]} + [IrCl_6^{2-}] - [NO_2]_0 - \frac{([Ir]_{tot} - [IrCl_6^{2-}])[H^+][HNO_2]}{K_4[IrCl_6^{2-}]} + [NO]_0 - [IrCl_6^{2-}]_0 \quad \text{(A12)}$$

The rate of production of NO_2 through step k_{-2} is defined as

$$dx/dt = 2k_{-2}[NO_3^-][HNO_2][H^+] \quad \text{(A13)}$$

Differentiation of eq A12 and substitution by eq A13 yield the rate law

$$\frac{d[IrCl_6^{2-}]}{dt} = 2k_{-2}[NO_3^-][H^+][HNO_2] \Big/ \left\{1 + [HNO_2] \times [Ir]_{tot}\left(\frac{K_3K_4}{[H^+]([Ir]_{tot} - [IrCl_6^{2-}])^2} + \frac{[H^+]}{k_4[IrCl_6^{2-}]^2}\right)\right\} \quad \text{(A14)}$$

Registry No. $IrCl_6^{3-}$, 14648-50-1; $IrBr_6^{3-}$, 18400-15-2; $[Fe(TMP)_3]^{2+}$, 17378-70-0; HNO_2, 7782-77-6; NO_2, 10102-44-0.

Contribution from the Research Laboratory for Nuclear Reactors, Tokyo Institute of Technology, Meguro-ku, Tokyo 152, Japan, and Department of Chemistry, Miami University, Oxford, Ohio 45056

Kinetics and Mechanism of Ozone Decomposition in Basic Aqueous Solution

HIROSHI TOMIYASU, HIROSHI FUKUTOMI, and GILBERT GORDON*

Received February 1, 1985

The kinetics of the decomposition of ozone have been studied in aqueous alkaline solutions by means of an accumulated stopped-flow method. In slightly basic solution ([OH^-] ~ 0.01 M; 1 M = 1 mol dm^{-3}), the reaction can be described by the following rate law involving first- and second-order terms in ozone: $-d[O_3]/dt = k_1[O_3] + k_2[O_3]^2$. The second-order term is not observed if a radical scavenger (Na_2CO_3) is present in the solution. In solutions of high [OH^-], the rate law changes markedly. The addition of Na_2CO_3 retards the reaction only in the latter stages, and the rate law becomes nearly first order in ozone as the concentration of added Na_2CO_3 is increased. The results provide kinetic evidence for the initiation step $O_3 + OH^- \rightarrow HO_2^- + O_2$, which corresponds to a two-electron-transfer process or an oxygen atom transfer for ozone to hydroxide ion.

Introduction

The current use of ozone in water treatment in the United States and Europe[1-6] has resulted in considerable interest in the chemical reactions and the analytical chemistry of ozone itself.[7-14] The decomposition and redox reactions of aqueous ozone have been reported in detail for more than 50 years. Many facets of the propagation steps in the decomposition of aqueous ozone have been elucidated as a result of a series of cleverly designed kinetic and pulse-radiolysis experiments by Hoigné, Hart, and co-workers.[15-19]

The details of the initiation step in the base-catalyzed decomposition of ozone have been proposed to involve one- and/or two-electron transfer (and/or oxygen atom transfer) involving O_3^-, HO_2^-, O_2^-, and OH as potential intermediates.[2,3,8,15-24]

A variety of early attempts were made to determine the role of ozone, and various orders (and combinations of orders) ranging from 0.5 to 2 have been proposed.[2,3,6,25-39] Unfortunately, many of the studies were not under comparable conditions (i.e. different ozone concentrations, pH, and ionic media, buffers present or absent, possible scavengers and promoters, etc.) resulting in "system-specific" rate constants. The early work of Taube and Bray[35] and others clearly points out the chain-reaction characteristics of the decomposition of aqueous ozone and notes the role of various scavengers such as formic acid, bromide ion, acetic acid, and others. The recent papers by Hoigné, Hart, and co-workers take advantage of scavengers such as acetic acid, carbonate ion, phosphate ion, and *tert*-butyl alcohol in order to define specific systems allowing for the elucidation of the various propagation and termination steps.[10,15-18,40-42]

This paper presents the results of accumulated time-resolved stopped-flow measurements that help to define the role of O_3^-,

* To whom correspondence should be addressed at Miami University.

(1) Symons, J. M. "Ozone, Chlorine Dioxide, and Chloramines as Alternatives to Chorine for Disinfection of Drinking Water"; presented at the Second Conference on Water Chlorination: Environmental Impact and Health Effects, Gatlinburg, TN, Oct 31-Nov 4, 1977.
(2) Peleg, M. *Water Res.* **1976**, *10*, 361.
(3) Zeilig, N. M. *J.—Am. Water Works Assoc.* **1983**, *75*, 34.
(4) Guinvarch, P. *Adv. Chem. Ser.* **1959**, *No. 21*, 416-429.
(5) Katzenelson, E.; Kletter, B.; Shuval, H. I. *J.—Am. Water Works Assoc.* **1974**, *66*, 725-729.
(6) Gorol, M. O.; Singer, P. C. *Environ. Sci. Technol.* **1982**, *16*, 377.
(7) "Standard Methods for the Examination of Water and Wastewater", 14th ed.; American Public Health Association: Washington, DC, 1975.
(8) Gordon, G.; Grunwell, J. "Proceedings of the Second National Symposium on Municipal Waste Water Disinfection"; Venosa, A., Akin, E. W., Eds.; United States Environmental Protection Agency: Cincinnati, OH, 1982; Vol. 18, pp 226-245.
(9) Bader, H.; Hoigné, J. *Ozone: Sci. Eng.* **1982**, *4*, 169.
(10) Hoigné, J.; Bader, H. *Vom Wasser* **1980**, *55*, 261.
(11) Tomiyasu, H.; Gordon, G. *Anal. Chem.* **1984**, *56*, 752.
(12) Straka, M. R.; Pacey, G. E.; Gordon, G. *Anal. Chem.* **1984**, *56*, 1973.
(13) Grunwell, J.; Benga, J.; Cohen, H.; Gordon, G. *Ozone: Sci. Eng.* **1983**, *5*, 203.
(14) Stanley, J.; Johnson, D. "Handbook of Ozone Technology and Applications"; Rice, R. G., Netzer, A., Eds.; Ann Arbor Science (The Butterworth Group): Ann Arbor, MI, 1982; pp 255-276.
(15) Staehelin, J.; Hoigné, J. *Vom Wasser* **1977**, *48*, 283.
(16) Fornl, L.; Bahnemann, D.; Hart, E. J. *J. Phys. Chem.* **1982**, *86*, 255.
(17) Buhler, R. E.; Staehelin, J.; Hoigné, J. *J. Phys. Chem.* **1984**, *,8*, 2560.
(18) Sehested, K.; Holcman, J.; Bjergbakke, E.; Hart, E. J. *J. Phys. Chem.* **1984**, *88*, 269.
(19) Sehested, K.; Holcman, J.; Bjergbakke, E.; Hart, E. J. *J. Phys. Chem.* **1982**, *86*, 2066.
(20) Ivanov, Yu. E.; Nikitina, G. P.; Pushlenkov, M F.; Shunkov, V. G. *Zh. Fiz. Khim.* **1972**, *46*, 2163.

0020-1669/85/1324-2962$01.50/0